Journal of Mediterranean Cities

2022, Volume 2, Number 1, pages 58–83

Fire and Explosion Machine Learning Model for the Port of Los Angeles - California Safety Code and NFPA for Fire-Break Zoning

* Ing. Arch. **Salvatore Polverino**

Training and Internationalization department, Order of Architects Planners Conservative Landscape Architects of Naples and Province, Italy
E-mail: formazione@napoli.archiworld.it; polverinosalvatore@outlook.com

ABSTRACT

A correlative Hazard case study of Los Angeles Port has been performed on a tremendous dock fire that occurred on 22nd September 2014 at the Wilmington Dock along with a proposed Machine Learning approach concerning remote sensing techniques, a time-related air quality survey, and port safety codes, which are assessed and based on a modern port governance emergency intervention. The methodology of this research embraces a possible case of high fire severity urban zoning of the Los Angeles Harbour, on the occasion of the severe application of Health and Safety Code Section 18930 by the State Fire Marshal to respond opportunely to the recent extensive ignition across California. Set rules, dispatched by LA Port System, are detected following a Landsat 8/OLI (Operational Land Imager) remote sensing-based geospatial comparison with ground-based air samples. In order to target opportunely risk barriers in favour of Oil Tankers and critical garrisons, an extensive pre-processing calibration of spaceborne datasets has been performed for enhancing minor changes on the platforms. Besides, intrinsic limits of the OLI definition do not permit appropriate accuracy of small-scale evaluations; a decision tree model has been therefore engaged by embracing high variance and low bias of these compensated datasets. In this manner, four Regions of Interest have been marked to strengthen the sub-samples of these features. The flexibility of RF computation delivers positive automation for the missing values, categorical and continuous values; on the other side time consuming and interpretability drawbacks, notice a disadvantage of the implementation in terms of computational training, validation, and testing. In defence of this intervention approach, an air-model geostatistical distribution carried out pixel values based on the pre-burn weighted trained model and finally ensembled to buffer protection zones, according to the Safety Code Section 18930 as an endorsement of further sustainable and financial liabilities that are vital parameters in the post-Covid-sars19 crisis and demonstrate growth limits of Ports as periodically issued to theirs Internal Consistency Analysis. The advisory assessment research moreover a hardware performance to support on-time prediction models, by listing variable dependent regressive accuracy samples.

ARTICLE INFO:

Article history:

Received: May 17 2022

Revised: June 22 2022

Accepted: July 10 2022

Available online: Aug 08 2022

Keywords:

International Safety Management Code, Digital forensics, Defense Architecture Framework, Fire Risk, Port Authority Competition

JOURNAL OF MEDITERRANEAN CITIES (2022), 2(1), 58-83

https://doi.org/10.38027/mediterranean-cities_vol2no1_5

www.mediterranean-cities.com

Corresponding Author:
Ing. Arch. Salvatore Polverino
Formazione e Internazionalizzazione, Ordine degli Architetti Pianificatori Paesaggisti Conservatori di Napoli e Provincia, Italy
E-mail: formazione@napoli.archiworld.it

How to cite this article:
Polverino, S. (2022). Fire and Explosion Machine Learning Model for the Port of Los Angeles - California Safety Code and NFPA for Fire-Break Zoning. *Journal of Mediterranean Cities*, 2(1), 58-83. https://doi.org/10.38027/mediterranean-cities_vol2no1_5

1. Introduction

1.1. Welding operations

Welding operations are essential for the logistic sector in the harbour settlements and are often executed by third-party companies. Special supervision (AF&PA. 2001. National Design Specification; AF&PA. 2003 Calculating the fire resistance of exposed wood members; American Institute of Timber Construction. 1984; An International Codes and Standards Organization. NFPA®30 2015; California code of regulations; California codes government code, section 51175-51189; Creosote Treated Timber, What you need to know, Wood Protection, West Yorkshire LONZA; White, R. H.; 2002; 2000 Emergency Response Guidebook) and flexibility of exercise are the main factors as follows the finding of the right carrier to move subsequently freights. Personal Protective Equipment (PPE) is a mandatory support for plasma cutter welding whose risk factors are highly highlighted by hot sparks, metal shards, shrapnel, and unintentional combustion. Regarding this last factor, it often occurs at shifting/restorage and lashing/unlashing operations in particular at the expense of unsorted goods that might not encompass sufficient shielding defence. As reported by local media, the dynamic of early ignition interested an important creosote coated timber volume triggered by a plasma cutter.

1.2. Government code

According to Section 18930 of the Health and Safety Code of California, pursued by the State Fire Marshal, building standards need to fulfil comprehensive space and structure defensibility in order to protect structures from the spreading of neighbourhood ignitions. In case of high fire severity, the jurisdiction is regulated upon Section 51182 by the Director of Forestry and Fire Protection. Consistent criteria of time-related factors such as this case study, buffer as indicators up to identifying the label of "State responsibility areas", in which the financial liability of fire prevention and suppressing are regulated by the Section 4125 (Repealed and added by Stats. 1965, Ch. 1144).

Monitoring and reviewing the effectiveness of process design and enforcement are led by the Director of Fire Protection whose quinquennial outcomes are synchronized with the general plan update; the results shall be reviewed under Sections 51178 and 51179. Fire-break zone are strategic drivers demanded to prevent the risks of high severity zones and are undertaken with a not less than 30 feet distance protection curtain along the property line, with regard to flammable goods and combustibles (API RP, 2021 - Management of Atmospheric Storage Tank Fires, 2006; NFPA 15 - Standard for Water Spray Fixed Systems for Fire Protection, 2007; NFPA 30 - Flammable and Combustible Liquids Code, 2012); insurance companies are not prevented from requiring wider buffer distances. High Severity Zoning was, besides, prompted for the first time by the Bates bill in response to the Oakland Hills Fire of 1991; the vertical hierarchy was hence a top-down policy-made in the prospective of duality between the Director of Fire Protection (top) and local jurisdiction (down). On behalf of the CAL FIRE Director, a final endorsement of evaluation is promulgated. New built or renewal constructions that are interested in structural damages by fire hazards shall obtain a certification of safeness that satisfies Section 51189 and relative insurance coverage.

In accordance with national and local building standards (City of Los Angeles. Department of Building and Safety; LADBS; County of Los Angeles, Department of Public Works Building and Safety Division; Disaster Management Areas, Cities, and Unincorporated Areas, Los Angeles County Operational Area; http://www.dec.ny.gov/regulations/regulations.html), a final inspection ratifies the appositeness; facades, whose implementation consisted of effective non-flammable usage of materials, shall be considered exempt by this evaluation. Transactions that are regulated under Section 1103 of the Civil Code, are subject to the Local Option Real Estate Disclosure Statement, as promulgated by the 1102.6a of the Civil Code, and the Natural Hazard Disclosure Statement as enacted by the Section 1103.2 of the Civil Code. A further shiftiness of hazard individuation shall lead to the Y/N marking by the transferor on the Natural Hazard Disclosure Statement, on behalf of technical attachments. Lands and waters of port

zoning are not subject to Section 51182 unless they include any habitat for endangered or threatened species by the state or federal government, parklands, and scenic values.

Because of the sensitivity of the Port Authority of California (Eleventh Coast Guard District Strategic Framework, 2019-2021) - five hundred meters as the crow flies not far away from the rising hills - fuel fossils storage has been included within FHSZ state-wide reflective fuels on the ground. Nevertheless, the limitations of the focus of FHSZ maps have demonstrated to undermine the adherence of insurers to fire protocols. To fill this gap, a Memorandum of Understanding (MOU) was signed by the Commissioner of the California Department of Insurance and the Director of CAL FIRE, in October 2007. Fuel storages express an important risk factor up to the direct correlation of the Hazard model itself, by designing a likelihood model that the area will burn over a 30-to-50-year period.

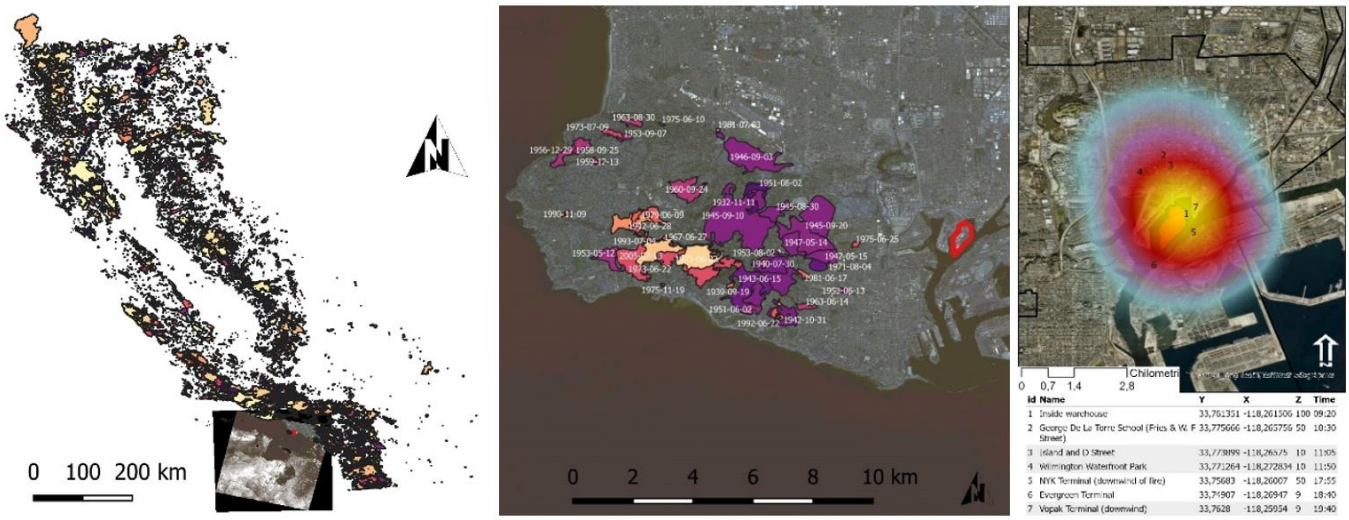

Figure 1. (a)California Fire Perimeters (map on the left), (b) LA Fire Perimeters (Map in the middle), and (c) SCAQMD inspection (Map on the right)

A crucial step for sustainability includes the possibility of productive entities being validated by insurance companies. Fire Hazard is the primary focus of the Fire Hazard Severity Zones (Frequently Asked Questions, FIRE HAZARD SEVERITY ZONES, FHSZ) maps, not Fire Risk.

Nevertheless, despite this ambiguity, the Fire Hazard model regulates the risk assessment, particularly for the fuel, slope, and fire weather, by considering the potential for damage based on fire spread. Mitigation protocols include, as stated in the previous paragraph, measures that comprehend defensible space, building design, ignition resistance building class, and ignition resistant construction technology. Managing risk is an iterative process finalized to deliver assistance as a key decisional for the whole management system. Its update faces off most recent technologies and the experimentation is fully capable of targeting human behaviour of external and internal criteria of corporate frameworks, nevertheless using remote data, spatially and temporally. Risk sources demand effectiveness and rapidity, especially for harbours in which combined storage can easily degenerate following cascading and cumulative effects (Ghasemi, A et al., 2017). The probabilistic methodology is hence a security measure and can be quantitatively computed, in the patterns of Likelihood Estimation.

The results obtained through modern approaches of computer vision algorithms demonstrate the possibility of getting deeper results and recovering obsolete grayscale values; the details quantify moreover a quantitative assessment which include highest accuracy. Finally, a ground model has been interpolated in order to get a visual comparison of both processes.

2. Methods

2.1. Port dock

The study case is searchable at Long. 33°45'35.3" Lat. 118°15'42.1" and interests 3,30 square kilometres; its area of ignition is extended to 1,21 sq. km. It lies behind the Wilmington-Harbour City urban system, at the boundaries of the following zonings: Light Industrial/M2, limited industrial/CM, M1, Community Commercial/C2, Public Facilities/PF, General/Bulk Cargo & Commercial/Industrial uses -non-hazardous/5A[Q]M3. As reported by Wilmington Waterfront Development Project Mitigation List (Transmittal 4), this bulk sector was provided with alternative evacuation and emergency routes which were addressed to immediate response during construction periods under the supervision of LAHD, LAFD, LAPD, LA Sheriff, and Fire Departments.

2.2. Image dataset

Image datasets are implemented in the research thanks courtesy of the U.S. Geological Survey.

2.3. Weather informations

On-ground events and dynamics are reconstructed by getting acquainted with personal witnesses and statements by major media agencies. National weather service and mesowest.utah.edu backed up relevant information already in 2014. Shapefiles are granted "without warranties of any kind, either express or implied, including without limitation, warranties of title or implied warranties of merchantability or fitness for a particular purpose" by the official portal of the City of Los Angeles. Surveys data are kindly distributed by the Los Angeles Fire Department. Four satellite scenes, selected before and after the hazard, present a modest cloud coverage but overall do not affect the case study. This fundamental condition has determined the start of the research.

Table 1. Ground observations at 09/22/2014 (Source: LA International Airport, KLAX)

Pressure	2.0 Wet bulb temperature	10.0m Wind Direction	Weather conditions
29.82 in	63.7 ° F	WSW	Clear

Table 2. Spaceborne observations (Source: National Aeronautics and Space Administration, NASA and United States Geological Survey, USGS)

Date	08-20	09-05	10-07	10-23
CLOUD_COVER	59.41	43.53	36.24	2.92
CLOUD_COVER_LAND	8.77	1.32	15.79	1.18

Table 3. Framework of research

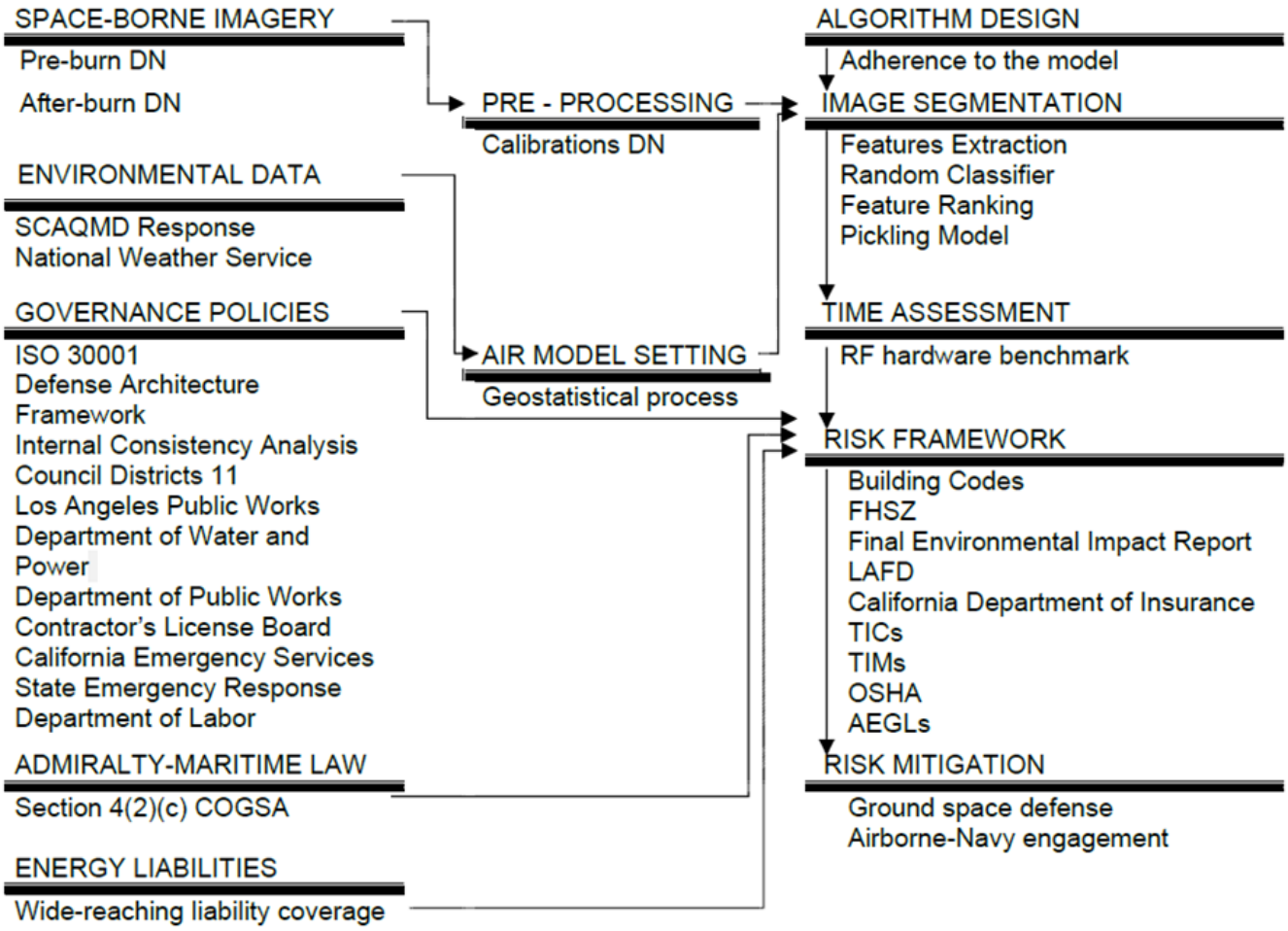

2.4. Ordinary Kriging

The response to fire at Port of Los Angeles (SCAQMD) evaluation started on the morning of 22nd September. Inspectors operated, since the beginning, at the Berth 177 by gaining air samples that were soiled by toxic hydrocarbons. The canisters, which were subsequently analysed, revealed elevated levels of Naphthalene due to the combustion of crude oil or coal tar associated with the stored timber stocks. In particular, the warehouse was reported to drive as a chimney of endless ignition. Furthermore, several inspectors were deployed in the neighbouring urban texture, whose instruments consisted of portable monitoring devices to assess particulate matter (PM) and hydrocarbons, by implementing gas chromatograph/mass spectrometer (GC/MS) measurements. The fine particulate matter was assessed to be larger than 2.5 microns and was mainly transported on the northwest side of the city by maritime winds under the clear sky.

The assessments were precisely vigilant over the maximum instantaneous activity due to the potential impacts on the community and embraced distant sites such as the George De La Torre School (Fig. 1c). This study strictly considers the toxic exposure of Naphthalene, whose heterogeneity consisted of benzene, and toluene compounds but disregards particulate matters measurements, estimated at 47 micrograms per cubic meter ug/m3, due to its chronic disturbance in the Los Angeles city. The measurements met the U.S. EPA standards regarding future comparisons against the National Ambient Air Quality Standards (NAAQS). In order to predict this Naphthalene distribution, an ordinary Kriging

method was preferred due to statistical usage of the same environmental Agency, with the estimation of prediction error rather than the Inverse Distance Weighting. Among seven correlated points (Fig.2), a prediction of the most probabilistic exposure along seven hundred meters was estimated, on behalf of true values, unbiased at each location, spatially autocorrelated, normally distributed, and stationary, by following the most stable algorithm of dispersion. Depending on how correlated the points are based on how distant they are located from one another, a correlation in known values was calculated and also predicted in further zones of the LA districts.

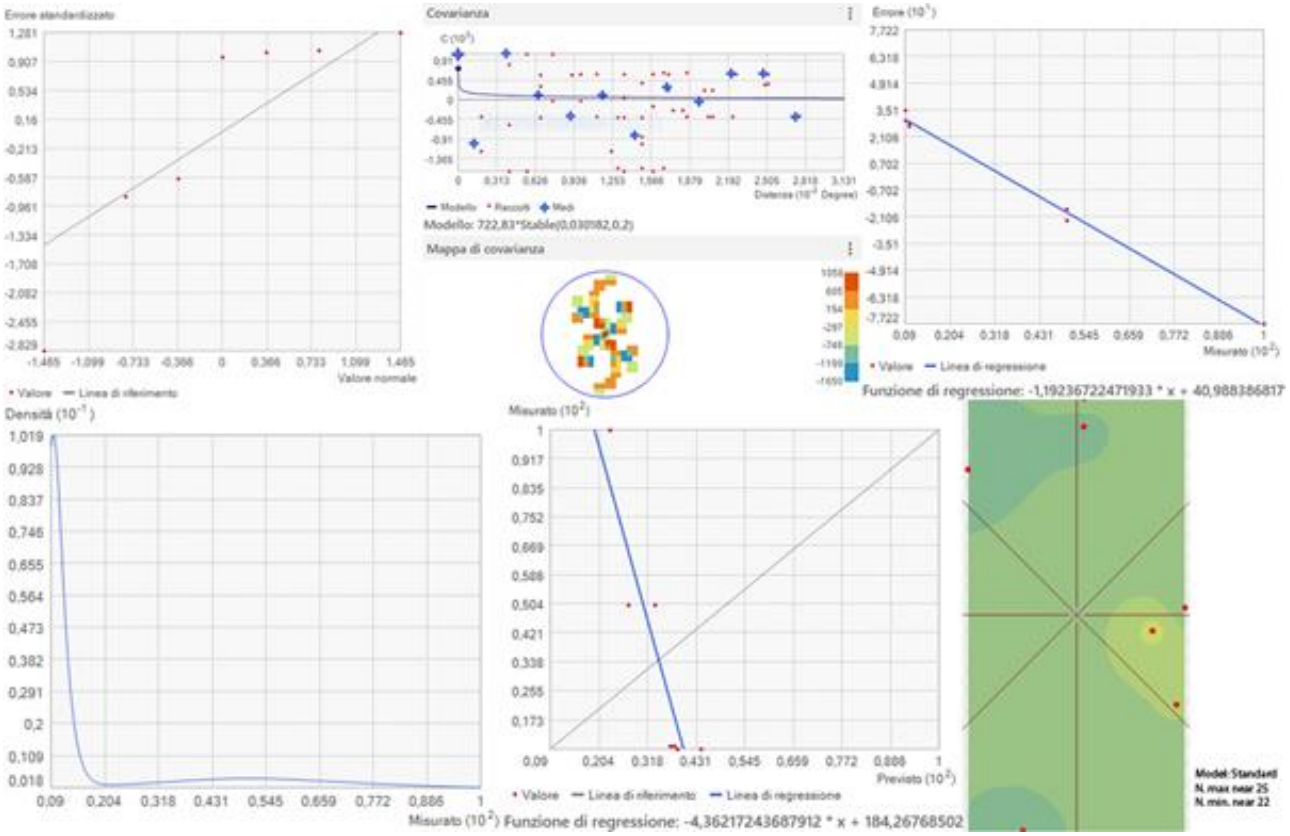

Figure 2. Kriging statistics

This linear-weighted averaging method was operated by the author under his own ArcGIS Pro license distributed by Esri. Additionally, as a result of the SCAQMD report, the local stationarity of the 7 surveys was guaranteed to start from the main emission located at Wilmington Dock, berth 177. Fire magnitude caused important structural collapses at the expense of the wharf and its Warehouse as declared and well-represented in the project description "Berths 177-178 Transit Shed Demolition Project, final initial study/negative declaration" prepared by: City of Los Angeles Harbour Department, Environmental Management Division (2016).

2.5. Radiometric and atmospheric image correction

As an essential part of radiometric and atmospheric image corrections, multiresolution (MR) remote sensing images require independent preservation of numerical details by each band (Benharrats F et al.; Brian L. et al.; Chander, G. et al., 2009; Landsat MSS, TM, ETM+, and EO-1 ALI Sensors). To deliver an adequate commutation into realistic environmental parameters with the purpose of overcoming

electromagnetic radiation (EMR) and subsequently comparing, four Landsat 8/OLI datasets prior to and successive to this hazard were considered.

The digital numbers (DN) were characterized by overall conformity of weather parameters except the third, whose cloud coverage nevertheless did not interest the region of study. Regarding extensive parameters, provided by the joint NASA/U.S. Geological Survey Landsat, an extended rescaling of values, was commuted into three physical units: at-sensor reflectance (Vermote E et al.) prior to the at-sensor radiance correction (%) (ToA), and the supervised Dark Object Subtraction (DOS) (Chavez, 1988, 1996; Gilmore S et al., 2015). This last was computed simultaneously with the Pan-sharpening refinement (Congedo L., 2016). In order to guarantee an enhancement of edge maps, panchromatic components were also included and subsequently with other morphological spectral, fused at the highest resolution. Low-definition multispectral MS sensors benefit from single panchromatic (PAN) bands at HR, in this case, 15 m, to re-enable consistency from spectral distortion, glaze and/or blur.

Table 4. Radiometric comparison

▷ Variable assigned to pixels		▷ At-sensor correction	
Rescaling 1 ToA	► Radiance correction	**Rescaling 2** ToA	►Reflectance correction
Require: DN **Values:** 1:M_p = Multiplicative rescaling factor (DN_reflect_mult_band_x) 2: Q_{cal} = Quantized and calibrated standard product pixel values (DN_cell_value) 3: $A\rho$ = Band specific additive rescaling factor (DN_radiance_add_band_x) **Ensure:** $p_{\Lambda'}$ cell value as radiance (Watts/(m^{2*}srad* µm))		**Require:** DN **Values:** 1: $p_{\Lambda'}$ = product of ToA reflectance without correction 2: Local sun angle = sin (θ_{se}) **Ensure:** p_{Λ} compensation of the solar irradiance Accurate reflectance calculations, can be also obtained by implementing per pixel solar angles rather than the scene center solar angle. Due to Landsat 8 products limitations, pixel solar angles cannot be currently obtained unless further calculations.	

$$p\Lambda' = M\rho * Qcal + A\rho \quad 1)a$$

At the early stage of the pre-processing research, an object-based method was considered essential because of the presence of determinate industrial elements that characterize this harbour sector. Otherwise from the manual radiometric correction, a semi-automatic DOS was performed simultaneously with the natural multi-band combination, to highlight urban features classification, i.e., industrial roofs and logistic elements.

A 4-3-2 pan-sharpened (6) set by four dates, was intrinsically considered less difficult to comprehend a harbour case unless an appreciable presence of vegetation for NIR composite was present. Besides, the study aims to deliver an adaptive guide case that can include also airborne/unmanned RGB/IR datasets operating in difficult conditions, i.e., smoke, fire, dusk, as support of time limited SaR intervention.

Table 5. Landsat metadata: (a) 08/20, (b) 09/05 (Source: developed by NASA and USGS)

	2014 - 08 - 20				2014 - 09 - 05			
	Radiance		Reflectance		Radiance		Reflectance	
Band	Gain	Bias	Gain	Bias	Gain	Bias	Gain	Bias
1	1.2265E-02	-61.32445	1.210700	-0.099980	1.2354E-02	-61.76958	1.210700	-0.099980
2	1.2559E-02	-62.79699	1.210700	-0.099980	1.2651E-02	-63.25281	1.210700	-0.099980
3	1.1573E-02	-57.86689	1.210700	-0.099980	1.1657E-02	-58.28692	1.210700	-0.099980
4	9.7593E-03	-48.79662	1.210700	-0.099980	9.8302E-03	-49.15082	1.210700	-0.099980
5	5.9722E-03	-29.86110	1.210700	-0.099980	6.0156E-03	-30.07785	1.210700	-0.099980
6	1.4852E-03	-7.42618	1.210700	-0.099980	1.4960E-03	-7.48009	1.210700	-0.099980
7	5.0060E-04	-2.50302	1.210700	-0.099980	5.0424E-04	-2.52119	1.210700	-0.099980
8	1.1045E-02	-55.22434	1.210700	-0.099980	1.1125E-02	-55.62520	1.210700	-0.099980
9	2.3341E-03	-11.67039	1.210700	-0.099980	2.3510E-03	-11.75511	1.210700	-0.099980
10	3.3420E-04	0.10000	1.210700	-0.099980	3.3420E-04	0.10000	1.210700	-0.099980
11	3.3420E-04	0.10000	1.210700	-0.099980	3.3420E-04	0.10000	1.210700	-0.099980

Table 6. Landsat metadata: (a) 10/07, (b) 10/23 (Source: developed by NASA and USGS)

	2014 - 10 - 07				2014 - 10 - 23			
Band	Radiance		Reflectance		Radiance		Reflectance	
	Gain	Bias	Gain	Bias	Gain	Bias	Gain	Bias
1	1.2572E-02	-62.86026	1.210700	-0.099980	1.2685E-02	-63.42480	1.210700	-0.099980
2	1.2874E-02	-64.36967	1.210700	-0.099980	1.2990E-02	-64.94776	1.210700	-0.099980
3	1.1863E-02	-59.31611	1.210700	-0.099980	1.1970E-02	-59.84881	1.210700	-0.099980
4	1.0004E-02	-50.01868	1.210700	-0.099980	1.0094E-02	-50.46789	1.210700	-0.099980
5	6.1218E-03	-30.60894	1.210700	-0.099980	6.1768E-03	-30.88383	1.210700	-0.099980
6	1.5224E-03	-7.61216	1.210700	-0.099980	1.5361E-03	-7.68053	1.210700	-0.099980
7	5.1314E-04	-2.56571	1.210700	-0.099980	5.1775E-04	-2.58875	1.210700	-0.099980
8	1.1321E-02	-56.60738	1.210700	-0.099980	1.1423E-02	-57.11576	1.210700	-0.099980
9	2.3925E-03	-11.96267	1.210700	-0.099980	2.4140E-03	-12.07010	1.210700	-0.099980
10	3.3420E-04	0.10000	1.210700	-0.099980	3.3420E-04	0.10000	1.210700	-0.099980
11	3.3420E-04	0.10000	1.210700	-0.099980	3.3420E-04	0.10000	1.210700	-0.099980

Unrectified OLI bands tend however to mislead and furthermore an accurate radiance adjustment benefits by picking up sun elevation values rather than solar zenith data since the latter might be affected by small anomalies (Yale University's Guide, 2013).
pΛ = (reflectance scale * cell value + reflectance offset) / sin theta

Table 7. Additional Landsat metadata (Source: developed by NASA and USGS)

	08 - 20	09 - 05	10-07	10-23
Sun elevation	60.79560196	56.99184431	47.39553813	42.23030775
sin	8,728846 E-6	8,385930 E-6	7,360443 E-6	6,721123 E-6

The Natural Color composite, (B04, B03, and B02 in the related red, green, and blue color channels), has surfaced the necessity of an Object-based image analysis whose iterative process has sought a merging and gradually filtering away process. The following supervised segmentation enhanced this coarse resolution and refined the augmentation by considering available references designed at higher resolution.

Figure 3. 0.630 – 0.680 - Red, 0.525 – 0.600 - Green, 0.450 – 0,515 - Blue (μ) at 08-20

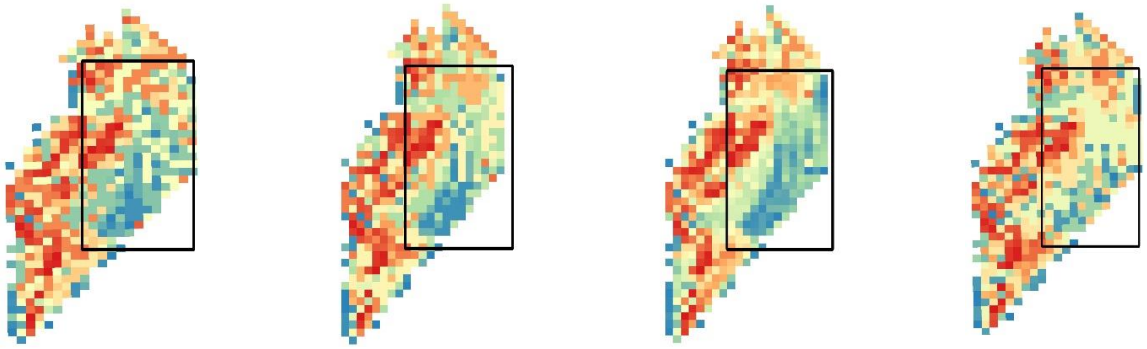

a *b* *c* *d*

Figure 4. (4-3-2) Spectral definition. a - 08-20. b - 09-05. c - 10-07. d - 10-23

2.6. Kernel

The advantage of a Gaussian kernel function, (Air Force Institute of Technology, 1989) which is modulated by a sinusoidal plane wave (Bhattacharya D. et al., 2009) and multiplied by a Gaussian function, introduces flexible possibilities for edge detection. Due to the multiplication-convolution property, the Fourier transform of the Gabor filter is the convolution of the Fourier transform of the harmonic function in the matter of a sinusoidal function and the Fourier transform of the Gaussian equation.

1) $g(x, y; \lambda, \theta, \psi, \sigma, \gamma) = \exp\left(-\frac{x'^2+\gamma^2y'^2}{2\sigma^2}\right)\exp\left(i\left(2\pi\frac{x'}{\lambda}+\psi\right)\right)$

2) $g(x, y; \lambda, \theta, \psi, \sigma, \gamma) = \exp\left(-\frac{x'^2+\gamma^2y'^2}{2\sigma^2}\right)\cos\left(i\left(2\pi\frac{x'}{\lambda}+\psi\right)\right)$

3) $g(x, y; \lambda, \theta, \psi, \sigma, \gamma) = \text{sen}\left(-\frac{x'^2+\gamma^2y'^2}{2\sigma^2}\right)\exp\left(i\left(2\pi\frac{x'}{\lambda}+\psi\right)\right)$

4) $x^{\wedge}{}' = x\cos\theta + y\sin\theta$

5) $y' = -\mathbf{x}\sin\theta + \mathbf{y}\cos\theta$

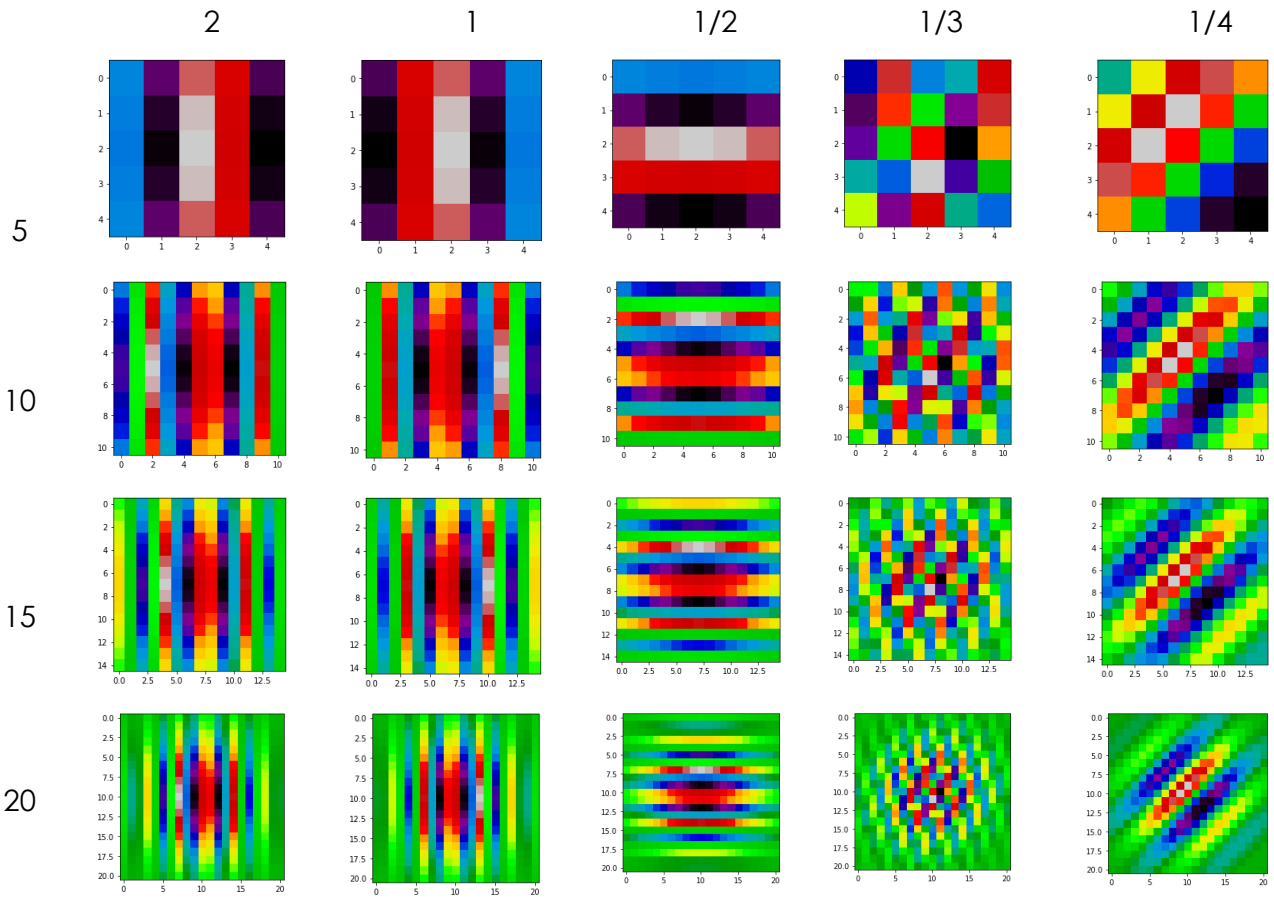

Figure 5. Pattern results

As prompted by a recent article (Ke Zhan, Hong You et al., 2020) the Gabor filter responses positively to the detection of translation, invariance to rotation and scale without requesting a high quality. In particular, the features determined by the Gabor filter, can derive from Gray-level images, and subsequently benefit of the implementation of the Random Forest Classifier (RF). Furthermore, its flexibility is well documented according to visual image research with regard of its similarity to the human visual system.

The scripting applied to Gabor filters has focused on five parameters: sigma, which establishes the size of the Gaussian envelope, psi, which determinates the phase offset, gamma, which is spatially necessary for the aspect ratio and adjusts the ellipticity, fx, or frequency of the sinusoidal component, nAngles, which characterize the number of filter orientations. The impulse response of these five parameters has delivered different combinations of a preliminary texture extraction. This strategy, organized in the matter of a filter bank, highlighted a numerous set of different sampling factors for a greyscale, which transmit the multi-resolution architecture of the Gabor pyramid.

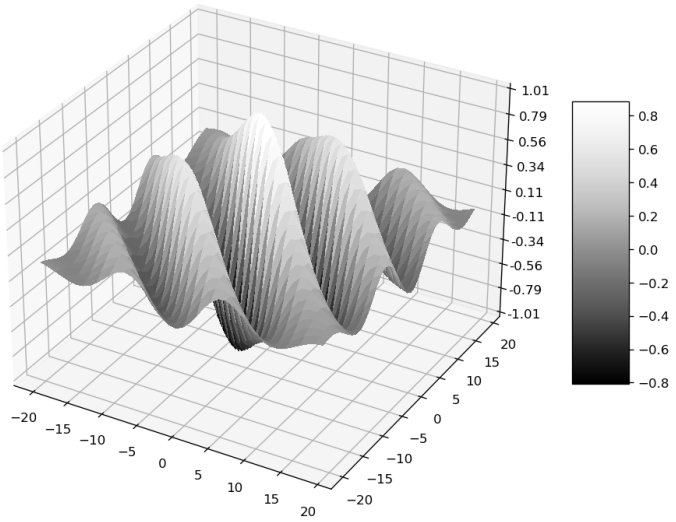

▷ wavelet factors

Algorithm 1 ▶ frequency model

Require:

1: λ = Wavelength of the sinusoidal component

2: Θ = The orientation of the normal to the parallel stripes of Gabor function

3: Ψ = phase offset of the sinusoidal function

4: σ = standard deviation of the Gaussian envelope

5: ɣ = The spatial aspect ratio ellipticity of the support of Gabor function

Ensure:

Ksize

Because of the horizontal patterns of the map image, it was considered to endorse as primary parameter the theta wavelengths for the orientation of the normal to the parallel. The edges were well represented with regard of theta = 1*np.pi/4 which has to be implemented towards future ortho-aerial applications.

A wide set of gabor computations was performed to enhance the texture analysis, edge detection, feature extraction.

Figure 6. Pattern. Gamma = 0.9 Sigma = 5 Phi = 0.8

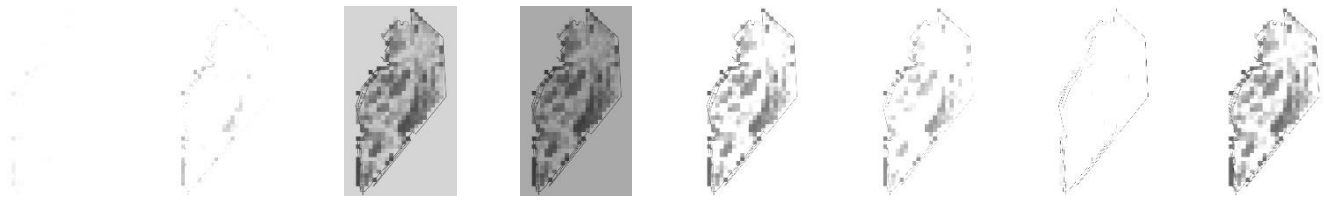

Figure 7. Feature extraction

2.7. Image Segmentation

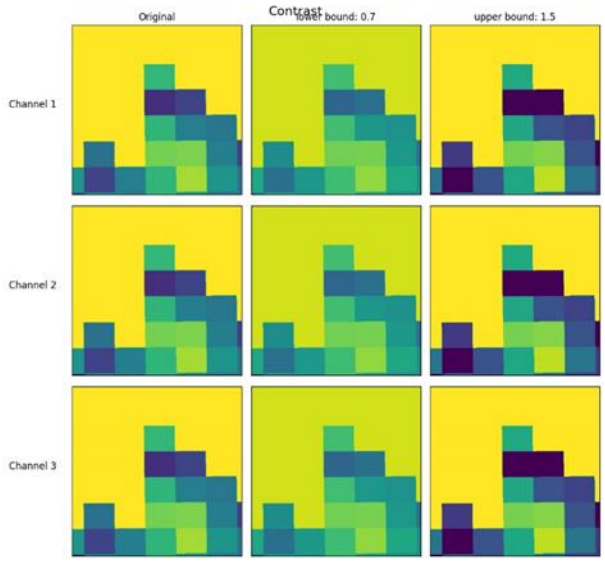

Figure 8. Contrast

Table 8. Inputs

Platforms	51367
Roofs	20748
Objects	53311
Oil Tankers Silos	24878

RF is a flexible algorithm (Xin-Ke Zhan et al., 2020) that delivers efficiency in the strict regime of low spatial references. Its minimalism and variety rely on both classification and regression methods. This combination of learning models, likewise multiple decision trees, is inclined to the fusion of different alternatives by cutting off the output variance. The training model in such a case was derived by the labelling of the 08-20 grayscale map whose base resolution was fixed in 2031*3673. The effective resolution, identifiable as squares, is much lower if scaled 1:1 (blocks to pixels). According to an extensive tagging of four regions of interest (ROI), a set of training examples, N= ((V1, V2, V3,…, Vn),y…), , whereby V indicates the feature of each sample and y the class label, was computed within the 2021-03-31, 15:18:25.

and 2021-04-01, 06:41.09 by means of a Carl Zeiss Microscopy GmbH Initiative, "From Image to Information". The node was entrusted to a Tesla K80, with 55 GB ram. The four labels that emerged in the following results, red for the objects, yellow for the platform, cyan for the roofs, and green for the oil tankers and silos, have determined the reading inputs as follows, in Table 9.

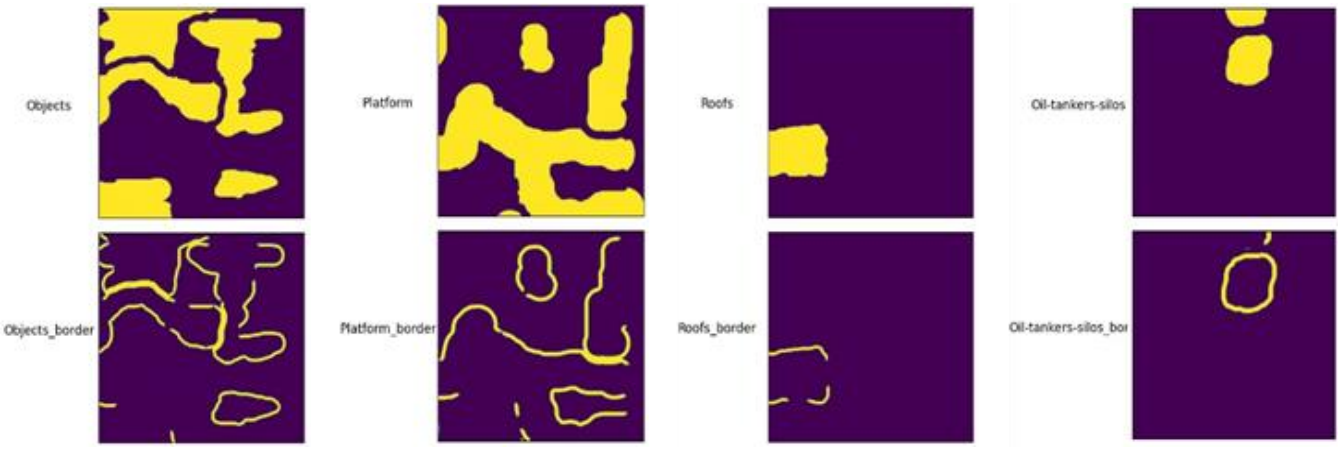

Figure 9. Edge detection

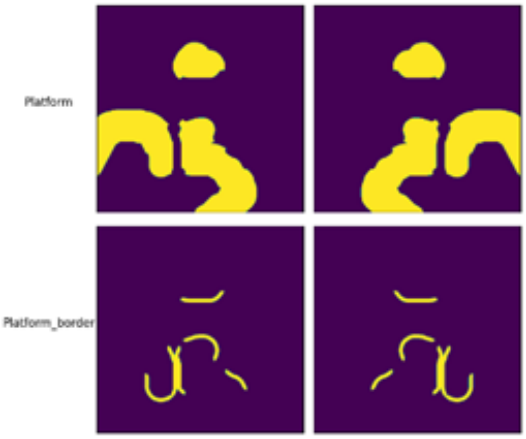

Figure 10. Flip left and right

Figure 11. Transpose

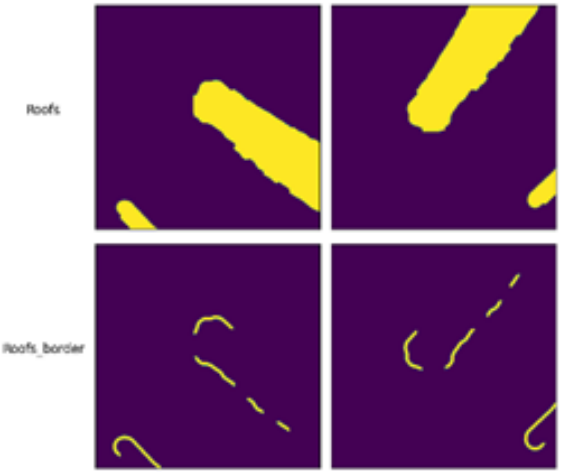

Figure 12. Rotation

In optimal conditions, a higher number of pixels determines divergent trends (Fig.13): for losses, both curves start at the top left and drop values at the bottom right; for accuracy, both curves start at the bottom left, rise rapidly, and constitute a form a plateau; likewise for both IOU curves.

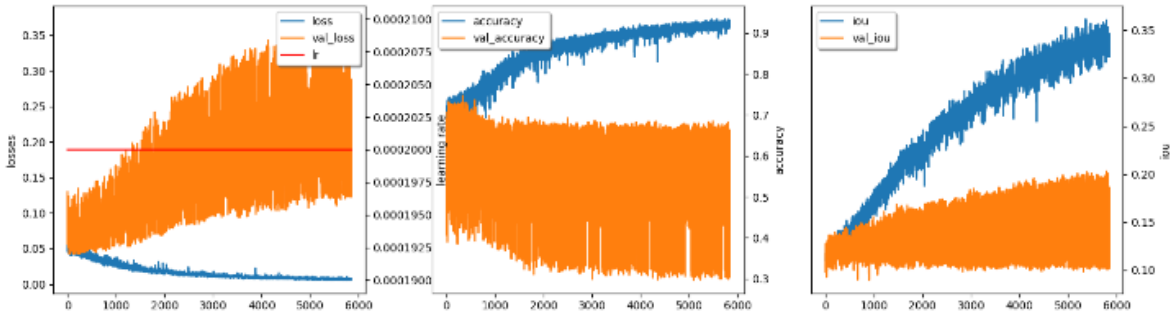

Figure 13. Training results. a – loss curves; b – accuracy; c – IOU index

2.8. Time assessment

Due to the nature of research, operating in crisis scenarios might require conditions that diverge from theoretical and indoor experimentations. By overcoming the initial underdevelopment of predictions, an increasing prediction benchmark regarding the hyper-parameterization of n_estimators and random_state is indicated as follows:

Table 9. Random Forest benchmark

N_estimators	Random_state	
10	42	*a*
9 min 51 sec A.T. 0.8347824591027939 A. 0.8189813086429848		
20	84	*b*
12 min 10 sec A.T. 0.8352199113611803 A. 0.8195540401870544		
25	105	*c*
13 min 46 sec A.T. 0.8352708506435664 A. 0.8197222737944989		
50	210	*d*
21 min A.T. 0.8353345247465491 A. 0.8201036479882678		
100	420	*e*
35 min 16 sec A.T. 0.8353508342536289 A. 0.8203194695882566		
200	840	*f*
1 H 3 min 15 sec A.T. 0.8353539621043018 A. 0.8203740952416699		
200	840	*g*
1 H 3 min 15 sec A.T. 0.8353539621043018 A. 0.8203740952416699		
400	1.680	*h*
1 H 57 min 13 sec A.T. 0.835354185522207 A. 0.8204250345012946		
800	3.360	*i*
3 H 51 min 05 sec A.T. 0.835354185522207 A. 0.8204022458851468		

The replicability of the number of trees was compromised after the "e" case by which the timing was not justified by the modest accuracy improvement. At the "I" attempt, the accuracy began to decrease. Besides, the scikit learn ML environment benefitted from additional other features matched with the data frame: Canny edge, Roberts edge, Sobel, Scharr, Prewitt, Gaussians with sigma equal to 3 and 7, Median and Variance with both sigmas equal to three.

Tested Hardware:

- Intel® Xeon® Processor E5-4650
1) 20M Cache, 2.70 GHz, 8.00 GT/s Intel® QPI
- Nvidia GeForce GTX 760
- 48 GB DDR-3 1600 ECC Ram
- 1 TB Samsung SATA III 850 EVO SSD

2.9. Machine learning geospatial comparison

To Assess an equal decision tree of the entropies that occurred under the four Geo-variations, the settings were addressed to the most convenient combination N-tree = 100, R-state = 420.

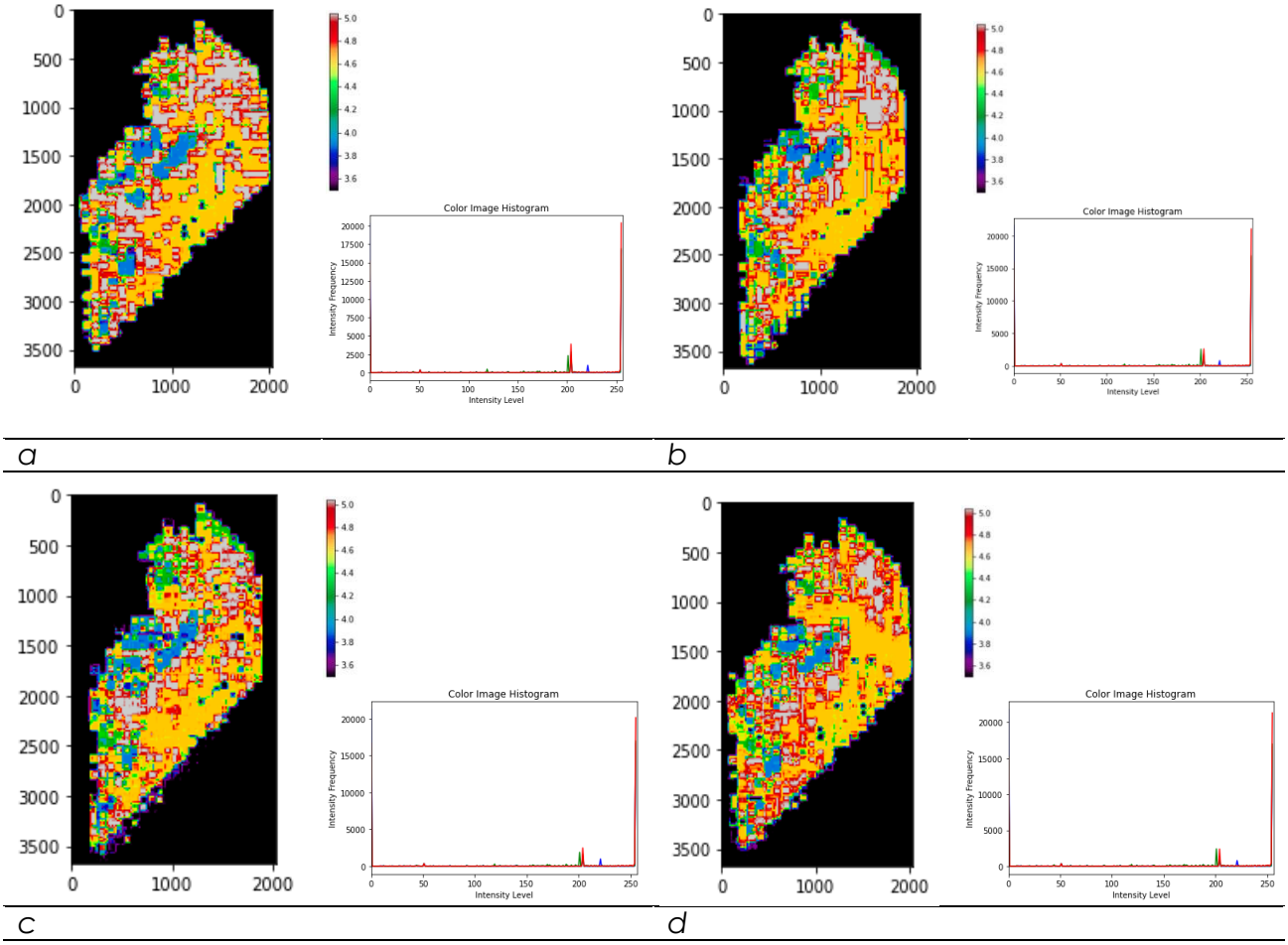

Figure 14. Random Forest Classification. a - 08 20. b - 09 05. c - 10 07. d - 10 23

The planned method generated four RF classification results, with an overall high sensitivity of 0.82031 % for the training result a, 0.764761 % for b, 0.81451 % for c, 0.78573 % for d.

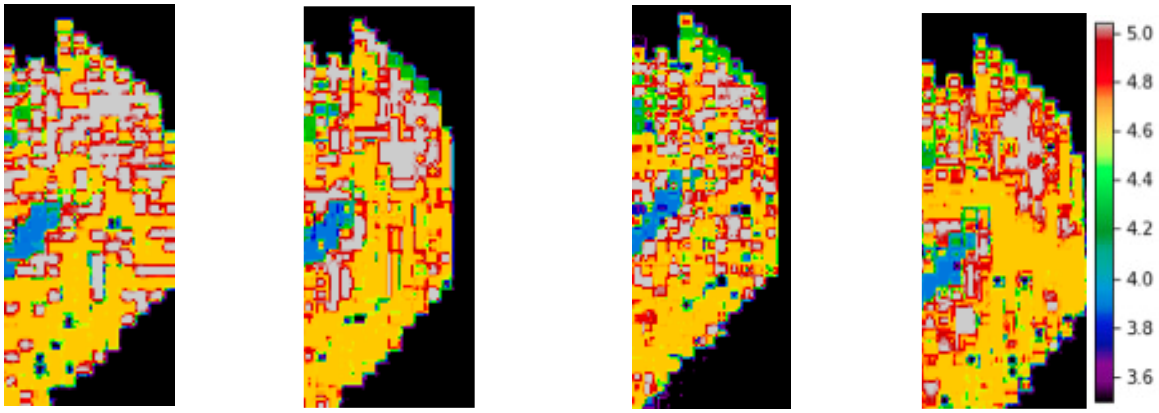

Figure 15. Entropies of fire at Wilmington dock. a - 08 20. b - 09 05. c - 10 07. d - 10 23

2.9.1. Hybrid augmentation

As a refinement of the Kriging air model, a superimposed model fixed at 2031*3673 was generated, by downgrading n-classes of the weighted average with neighborhood points, a – b. The research acquired a wide and precise strengthening based on the RF training: by partitioning the set of all points in X which maintain a distance inferior to the other sites Pj. J is any index dissimilar from k (c):

1) $R''k'' = \{x \in X \mid d(x,P''k'') \leq d(x,Pj) \text{ for all } j \neq k\}$

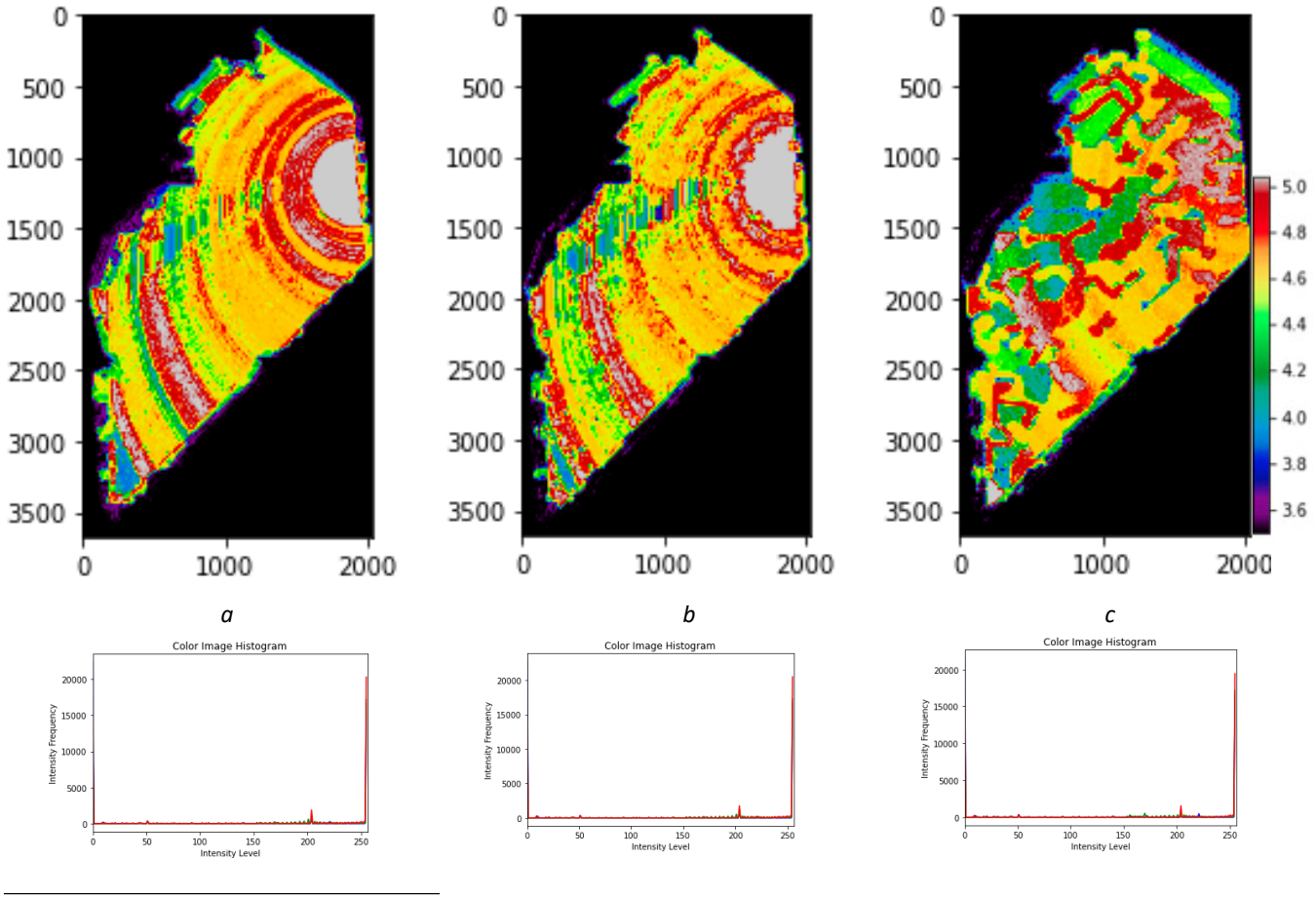

Figure 16. Superimposed model. a – below n. b – above n. c - decomposition of the air set

3. Results and discussion

As stated at the premise of the article, the study delivers a machine-learning-based prediction model whose criticalities can anticipate demands of multipurpose shifts in hazard scenarios. To conclude, a review insight has mediated among different research articles involved in the demand predictions of risk scenarios. As discussed by a recent article (R. Jenkins, J. Lunday, et al., 2020) on the subject of great-power conflicts (Army Field Manual No 3-9. Potential Military Chemical/Biological Agents and Compounds, 1990; Clive K., 2006; Herman S. Wolk, 1962), machine learning has been completely recognized as essential by its implementation in military scenarios: between 2001 and 2014, more than 4,500 U.S. military medevac were coordinated with regard of its accuracy.

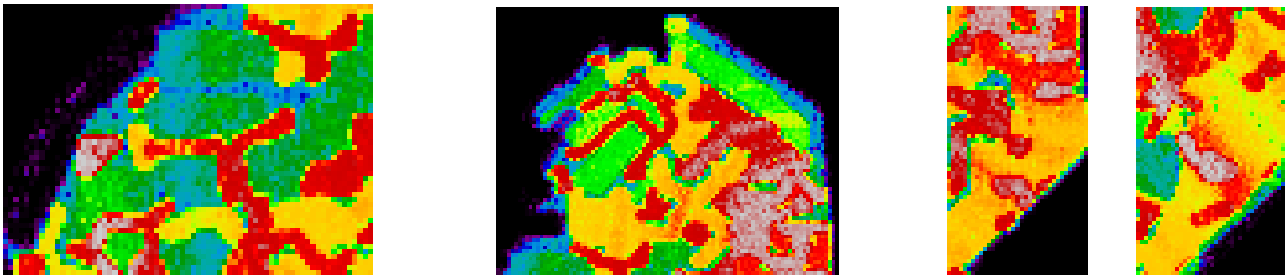

a *b* *c* *d*

Figure 17. Risk augmentation. a – Shore Terminals. b - Access. c, d – Platform

The report, obtained from extracted logistical points, has guided the allocation of first aid and evacuation assets as intended to permit the quickest and safer search and rescue operations. Professional aerial firefighting assistance has subsequently benefitted from the military protocols ruling steady-state combat operations through the implementation of specialized equipment such as infrared cameras, hoist/lifting possibilities, projectors, applied robotics, which ensures full compliance within the degraded visual environment as regulated by the National Fire Protection Association (NFPA). Following the extension of health and safety policy, a large-scale fire safety management research (Wong, Xie, et al., 2014) has underlined the necessity of tailoring ad hoc approaches that correspond not applicable responsibilities for each different issue.

Ensuring safe evacuation and enclosing in partitions fire and explosions risks have determined the resilience of multipurpose docks. Containerization in particular demands own safety zones to assist the transferring of intermodal freight transport.

The Wilmington dock has waited two years until the demolition project of berths 177-178. This delay has consequently addressed further costs which are related to the utilization of traffic randomness. Its disseverance is inclined to the restraint of limited areas that may benefit by the garrisoning of the Oil Tankers sector from even more fatal risks (a). Financially, informatic models have outlined default risk under berth-based tasks, i.e., ship turnaround time, waiting time for bulk cargoes, containers, and trucks (Mir A. Wahed, Faghri, Li).

Due to the heterogeneity of the traffic utilisations, an informatic model has been performed in order to simulate supply chain tasks (ship turnaround time, waiting time for bulk cargoes, containers, and trucks) that assist berths maneuvers. The research stimulated the perceptiveness by listing a set of equations prompted by the United Nations Conference on Trade and Development (UNCTAD), held on 1985.

The current literature is resampling important theoretical models in conjunction with the reinforcement of hardware and information validation that has brought together premium estimation in the fire insurance along with random variables, e.g. severity, occurrence date, claim date) by predicting severity results using semiparametric bootstrap.

Table 10. Sectors and likelihood values

Driver	Function	Contingency	Free zone	Access
S Fries Ave Warehouse	Industrial/Commercial	Sufficient	Average	Average
Pasha Stevedoring	Breakbulk cargo	Sufficient	Resilient	Average
Pier A St	Marine related	Average	Average	Average
Shore Terminals LLC	Petroleum Division	Resilient	Resilient	Resilient
Falcon St	Chemical related	Resilient	Average	Average

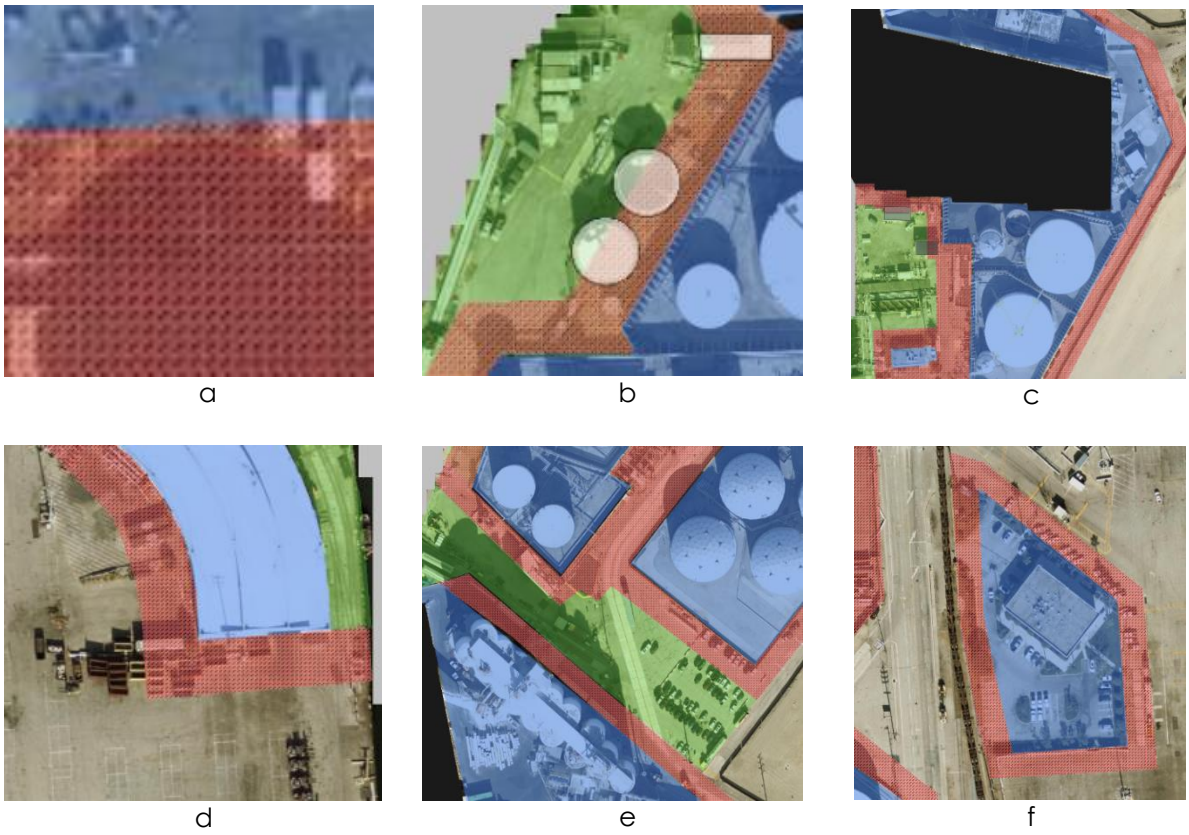

Figure 18. Buffer zoning: Blue as a free zone stands for normal conditions whereby the operations are guaranteed. Red as fire barriers, gateways. Green as checkpoints from the sea to evacuate the survivals

The study finally ensures adaptability of military implementation accompanied by special jurisdiction to be applied in Admiralty and Maritime Cases (R. Force, 2013) along with Defence Transformation capabilities (Kerr, Cambridge. 2006) with special mention of strategic national assets and Potential Military Chemical/Biological Agents and Compounds (Department of the Army, Navy, Air Force, 1990).

4. Conclusion

This proposed methodology lastly illustrates a resilience-based bibliography subscribing to the applicability of the prediction model to other regions in the Mediterranean basin, outside of California,

specifically referring to Harbourscape's core and its revolving zoning encompassing different examples through space and time.

This spatiotemporal identification of a defensive framework in the Mediterranean context has been recently corroborated crosswise a documental and historical investigation, conducted by a joint Italian-Arabic-Spanish program, also signed by the transnational academic agenda of the fifth issue of the International Conference on Fortifications of the Mediterranean Coast (FORTMED, 2020).

By enabling a Culture and Management census of defensive landmarks in the Mediterranean basin, academics acknowledge the support for the inseparable affiliation developed through time, in the dualism of both marine and terrestrial harbour scape (Moretti, B., 2017), as a result of cultural contrasts and positive alliances.

This primary value in the fortified coastal landscape (Cacudi G., 2020), was highly dependent on terms of internal core resilience to give a hand up in the ad of the architectural emergencies that occurred in the interior of the defensive perimeter, and thus, the necessity to assembly watertight compartments.

The article highlights the outstanding constructive superiority with the upgrading of newer walls techniques, and secondarily, the importance to hire religious orders of which talented persons capable to live in restrained core environments, hence preserving the privacy and military vulnerabilities of such military standpoints accomplished by own skilled workers; this dedication mastered the preservation of the elite moral group's integrity along the Italian peninsula (Cornell Per., 2020), without interfering the noisy environment of the city.

As the leadership of peace and prosperity in the Mediterranean was established, the fortified core, that constituted the main landmark of settled feudalism (Cecamore S., 2020), with its new revolving area, currently identified as retro-port as the proposed Machine Learning application conclusively discusses, began to function as a check-point with regard to trades, census's activities, and custom fee application; the urban sectorization in watertight compartments was thus extended in the peripheric ring of the fortified complex (Mollo G. et al., 2020), lastly emptied of its counter siege function (Molteni E. et al., 2020) by encompassing the allocation of institutional representation and core-warehouses.

The visual hierarchy constituted another infrastructural driver demanded from the builders; whether the natural cliffs did not consent to establish standpoints or not, the volume also includes the case regarding the erection of towers along the Tyrrhenian and Ionian coastlines, actually, Calabria of Italy, that successfully functioned as a traffic light tower chain, and that also permitted to operate and to take decisions by staying within the own fortification boundary, namely aree di incastellamento (Canonaco et al., 2020), a constructive matrix to the historical-functional one (Canonaco et al., 2018); this Mediterranean harbourscape is identified by the authors as paesaggio classico (Caniglia, 2017), that was particularly researched by the European aristocracy across the 18th-19th centuries in the occasion of the Grand Tour campaign.

This barricade-and-rescue narrative insists on an ancient territorial quality of harbourscape at present investigated (Moretti B. 2016-17), that has, in relatively recent times, undoubtedly inflated risk assessment frameworks commuted in the civil sector, as the newer European legislation, Seveso II Directive (Delvosalle C. et al., 2005), that has recognized the hazardous dualism between harmful installations and vulnerable residential areas, with the purpose of dismissing the adverse effects derived from industrial sites and susceptible suburban areas (Christou M., 1999).

From a core-system point of view, the article insists on the separation of distances as a safety protocol resulting in land use planning's (LUP) harmonization, backed up by the garrisoning of major accident hazards in the example of the Azote Fertilisant (AZF) factory's aftermath in Toulouse, considered by the French Authorities and the Joint Research Centre (JRC).

Article 12 of the Seveso II Directive, resulting from the Lille conference and the Amendment Directive 2003/105/EC introduced a new set of principles on a modern systematic basis, within a core area and a peripheral health effect threshold, for which the practitioners are called to propose their inventiveness, across four methodological approaches: a) deterministic strategy with the implicit judgment of risk, b) consequence-based approached, c) risk-based (or "probabilistic") approaches, d) semi-quantitative approaches.

In the Italian action program, from a national and legal perspective, the Port System Authority (AdSP) regulates the Port scheme, as declared by the legislative decree of 4 August 2016, and its related judicial police functions, addressed to public rescue service and fire prevention and extinguishing, also depending on the Ministry of the Interior, are ruled by the National Fire Brigade Corps (in acronym C. N. VV. F. and abbreviated as VV. F.) a highly equipped and civil body of the Italian Republic.

Its observances are mandatory to legally operate across a multi-scalar leadership, that has guaranteed security of institutions though the time, in the execution of economic, productive, and logistical survival assistance in the aftermath of internal or international crises; one research governance body, specifically contributing with the Italian fire-fighters, is the Istituto Nazionale Assicurazione Infortuni sul Lavoro (INAIL), with its Department of technological innovations and safety of human plants, products, and settlements.

A recent book released in 2020 (RISCHIO INCENDIO ED ESPLOSIONEIN EDILIZI, Prevenzione e procedure di emergenza, INAIL 2020) has summarized the most updated state of the art in terms of procedures and prevention in case of emergency.

Back to this manuscript's issue, the early hazard stage, developed in this tremendous fire threat that occurred in 2014 at Los Angeles's Wilmington Dock, was identified by forensics in the matter of sparks; according to INAIL guidelines, chapter 1, soldering works are included in the group of open flame activities, even though temporary, thus occurring in ambiances that are not equipped by proper shielding and smoke detection.

The aggravation of such an altered risk profile is entangled by unawareness and antiquity of the built environment heritage or general restoration. Thus, the book dispatches a list of best practices that acknowledge the current issue to prevent the usage of this Machine Learning research:

- To carry out welding operations outside, if this is not possible to ventilate abundantly the premises before, during and after the work;
- To remove all flammable materials in an area greater than 10 m around the welding point;
- If this is not possible, carefully cover everything with suitable and non-combustible devices;
- To do not carry out welding operations if there is a possibility that sparks will strike combustible or flammable material;
- To protect yourself and others from sparks and hot metal;
- To Be careful, sparks and hot materials resulting from the welding process can easily
- To enter through small cracks and openings and move to adjacent areas;
- To beware of possible fires (always keep a fire extinguisher available nearby);
- To be careful, as welding operations are carried out on ceilings, floors, retaining walls or
- To divide objects that can cause fires on the opposite side;
- To do not carry out welding operations on containers previously used for storage of fuels or closed containers such as tanks, cans or pipes, unless these are prepared appropriately and remediated;

- To do not carry out cutting operations on closed containers such as tanks and bins;
- To connect the work cable to the workpiece as close as possible to the welding area in order to
- To avoid that the welding current has to travel long distances, even out of sight, as this can cause electric shock and fire hazard;
- To do not use the welding machine to defrost pipes;
- To do not weld where the atmosphere may contain flammable dust, gases or vapors (such as those of gas);
- To do not weld cylinders, pipes or containers under pressure;
- If it is necessary to carry out operations on metal pipes, move away from them, along the their path, combustible or flammable materials eventually in contact.
- To care must be taken if these are wrapped with combustible insulating material;
- To wear non-oily protective clothing such as: leather gloves, heavy shirt, trousers without lapels, high shoes and a headdress;
- To do not place the machine on combustible surfaces;
- To remove all fuels, such as butane lighters or matches, from yourself before starting any welding operation;
- For Fire and explosion risk in buildings :
- once the work is completed, inspect the area and check for the absence of sparks, burning embers and flames;
- make sure that the escape routes are kept free and usable even during the operations welding;
- use only the correct fuses or safety switches;
- do not increase it in a way.

In the Mediterranean harbourscape, one introduces three hazards that occurred over the last years: in Italy (1), the cases of Ancona and, (2) the Torre Piloti of Genova, in the middle east (3), the Beirut blast.

The harbour of Ancona (1) was interested in a large fire with three powerful explosions identified in the commercial zone, whose ignition burned down three hangars. As reported by the technical dispatch (INCENDIO AL PORTO DI ANCONA DEL 16.09.2020; REPORT FINALE Sistema nazionale per la Protezione dell´ Ambiente), this methodology of capturing air-ground samplings, in the immediate hours of the event, 02:00 A.M., is equivalent to the Los Angeles report of research. The quantitative assessments also included metals and waters samplings and are eligible to repeat similar research outputs demonstrated in the case study of the paper.

A thesis on this harbourscape's heavy-industrial zoning has been highlighted in the article "The soundscape of the sectorization of Ancona Port" (1), whereas the research has been conducted with respect to ISO/TS 12913-2 technical specification: Soundscape Approach in the Seaport of Ancona et similia (Di Loreto et al., 2022; Cain R. et al.; Davies, W. et al., 2013).

The second scenario (2) occurred on the 7th of May 2013, regards the crash aftermath at the Port of Genova, with similar dynamics to the issue prompted by this paper's research: the merchant ship Jolly Nero, assisted by the tugs, was escorted out from the Port of Genoa. Due to human mistakes, it impacted from the stern against Molo Giano, and its standing Piloti Tower (Pilots Tower) (VTS). The over 40,000 tons of tonnage of the ship and the speed of approximately three knots, triggered off a tragic kinetic reaction.

Search and recovery (SaR) operations were perpetuated in the following 10 days of uninterrupted access by the firefighters (RISCHIO INCENDIO ED ESPLOSIONE IN EDILIZIA, Prevenzione e procedure di emergenza, INAIL 2020). Temporary Health care cores were allocated in shifts of 12 hours under the 118 Ligurian services. Tragically, the operations stopped with the discovery of the ninth victim still missing from the appeal.

In the third instance, an extremization of psychological and physical damage is represented (3) by the Beirut aftermath (Barrington L., 2017) of which a nuclear-like explosion (Chami, N. et al., 2021) dismantled the Port Authority of Beirut and its neighbourhood, in a radius of 4 km. By mentioning this latest scenario, the authors report the impossibility to ever return to "normality" with a significantly altered perception of safety and chronic stress.

The authors distribute a qualitative scheme of a survey of trauma-coping mechanisms and their time-related slower recovery patterns (El Sayed et al., 2015), previously conducted in 2000 by Steil & Ehlers for Beirut, analog to the case of the Gaza Strip.

Additional studies on the Beirut blast, testified an aggravating and chronic pain of accumulated alertness, stoically tolerated by its citizenship, and turned out to be an unsolved conciliation for Architects, Engineers, and Psychologists, to solve this current somatization also in economical (Beirut Post Blast Reconstruction) terms: the authors considered the real estate decadence of the city because of the SOLIDERE ("Société Libanaise pour le Développement et la Reconstruction du Centre-ville de Beyrouth") aggressive urbanization, in the decades gone by due to the war, collectively deteriorated with the socio-economic Lira inflation and its rampant social gap.

With this premise, this third scenario, proposed as avant-garde urban example in terms of independence of the Port core system, has been entangled in rivalry with the Beirut Central District. This political choice of urban assignment, merely identified as the inner island, was since the early concept assumed as controversial and repetitively reclaimed by urban citizenship, with a proposed masterplan that consumed 37% of the concerned area herewith labelled as new developments, 31% for Infrastructure and highways whereas 12% only was for retained buildings.

The new reconstruction of Beirut shall avoid this missing chance of reconnection between the Port and the city and thus, according to decree No.194/2020, which also blocked any future SOLIDERE replica to preserve what remains of the last architectural heritage: we consider that during the dismantling of the overall present war ruins, the 80% of buildings formerly scheduled in the safeguarding protocol promised by SOLIDERE were on the contrary pulverized (UN-Habitat, 2020).

Indeed, the computation of defense-oriented buffering zones through a Machine Learning methodology is an eligible investment to harmonize even annihilative bombing countereffects at the expense of vulnerable facilities, as a guidance to a masterplan designation of barriers and fords. Regarding the human lives, one suggests the conjunction with reinforced underground infrastructures that are proportionated to shelter citizens and traffic vehicles, in respect of reassignment of promenades and events on the surface, impacting positively on cultural memory having relevance on the chronic numbness and avoidance coping-mechanism.

Acknowledgements
The scope of this quantitative research is aimed to enlighten the modern approach of the image- and remote-sensing applications in favour of sustainable planning of port areas, with regard to engineering safety and Search and Rescue operations and as novel research in the Port Authority strategic planning. The author gives proper credit as enlisted in the references section.

Data availability statement
The original contributions presented in the study are included in the article/supplementary material, further inquiries can be directed to the corresponding author/s.

Ethics statements
Studies involving animal subjects: No animal studies are presented in this manuscript.
Studies involving human subjects: No human studies are presented in this manuscript.
Inclusion of identifiable human data: No potentially identifiable human images or data is presented in this study.

Conflict of Interests
The author declares no conflict of interest.

References

American Forest & Paper Association, (2001). National Design Specification (NDS) for wood construction. American Wood Council. www.awc.org

American Forest & Paper Association, (2003). Calculating the fire resistance of exposed wood members. Technical Report 10. American Wood Council.
https://www.portlandoregon.gov/bds/appeals/index.cfm?action=getfile&appeal_id=8200&file_id=1958

Veronin, C. (1990). OPTICAL IMAGE SEGMENTATION USING WAVELET FILTERING TECHNIQUES, Air Force Institute of Technology. https://apps.dtic.mil/sti/pdfs/ADA230584.pdf

Al-Hajj, S., Mokdad, A., & Kazzi, A. (2021). Beirut Explosion Aftermath: Lessons and Guidelines. Emergency Medicine Journal 38, n. 12: 938–39. https://doi.org/10.1136/emermed-2020-210880.

American Institute of Timber Construction, (1984). Calculation of fire resistance of glued laminated timbers. Technical Note No. 7. http://www.aitc-glulam.org/

An International Codes and Standards Organization, (2015). Flammable and Combustible Code. https://www.nfpa.org/codes-and-standards/all-codes-and-standards/list-of-codes-and-standards/detail?code=30

American petroleum institute, (2021). Management of Atmospheric Storage Tank Fires. API Publishing Services. https://www.api.org/

Barrington, L. (2017). Beirut Redeveloper Solidere Struggles Through Lebanon's Turmoil LisaBarrington, viewed 4 March 2021, https://www.reuters.com/article/uk-lebanon-economysolidere-idUKKBN1E60UH

Benharrats, F., & Mahi. H., (2020). Surface Solar Radiation Modeling from Landsat 8 OLI/TIRS Satellite Data. In 2020 5th International Conference on Renewable Energies for Developing Countries (REDEC), 1–4. Marrakech, Morocco, Morocco: IEEE, 2020. https://doi.org/10.1109/REDEC49234.2020.9163851.

Bhattacharya, D., Devi, J., & Bhattacherjee, P. (2013). Brain Image Segmentation Technique Using Gabor filter parameter. School of Electrical Engineering. Volume-02, Issue-09, Vel Tech and SR Technical University. American Journal of Engineering Research.

Markham, B., et. al., (2014). Md Obaidul Haqued Radiometric Calibration and Stability of the Landsat-8 Operational Land Imager (OLI) NASA/GSFC, Greenbelt, MD 20771. Proceedings Volume 9218, Earth Observing Systems XIX. https://doi.org/10.1117/12.2063159.

Giovanna, C. (2020). Gallipoli nel paesaggio fortificato del Mediterraneo. In X, 537–44. Universitat Politàcnica de València. https://doi.org/10.4995/FORTMED2020.2020.11477.

Rebecca, R., Jennings, P., & Poxon, J. (2013). The Development and Application of the Emotional Dimensions of a Soundscape. Applied Acoustics 74, n. 2: 232–39. https://doi.org/10.1016/j.apacoust.2011.11.006.

Caniglia, M.R. (2017). L'Italia meridionale nei disegni di Edward e Robert-Henry Cheney (1823-1825), in Belli, G.; Capano, F.; Pascariello, MI.I, eds., La città, il viaggio, il turismo. Percezione, produzione e trasformazione, CIRICE, Napoli, pp. 695-701.

Canonaco, B., Bilotta, F. (2018). Analisi e conoscenza del sistema fortificato della costa dell'alto Tirreno Calabrese, in FORTMED 2018. Defensive Architecture of the Mediterranean: Proceedings of the International Conference on Modern Age Fortification of the Mediterranean Coast, Politecnico di Torino, Torino.

Stefano, C., (2020). Traces of a fortified hamlet. Iconography and urban development of San Valentino in Abruzzo Citeriore. In X, 569–76. Universitat Politàcnica de València. https://doi.org/10.4995/FORTMED2020.2020.11390.

Rizk, Y., Nael, C. (2021), Beirut Post Blast Reconstruction. Academia Letters. https://doi.org/10.20935/AL2107.

Chavez P. S. Jr. (1988). An improved dark-object subtraction technique for atmospheric scattering correction of multispectral data. Remote Sensing of Environment. 24(3):459-479.

Chavez, Pat S. Jr. (1996) «Image-Based Atmospheric Corrections - Revisited and Improved». Photogrammetric Engineering and Remote Sensing 62: 1025–36.

Christou, M. (1999). Analysis and Control of Major Accidents from the Intermediate Temporary Storage of Dangerous Substances in Marshalling Yards and Port Areas. Journal of Loss Prevention in the Process Industries 12: 109–119. doi: https://doi.org/10.1016/S0950-4230(98)00043-6.

City of Los Angeles, (2021). Zoning Code Manual and Commentary (Fourth Edition), Department of Building and Safety (LADBS). https://www.ladbs.org/

Kerr, C. (2006). A framework for strategic military capabilities in defense transformation. The 11th *International Command and Control Research and Technology Symposium* (ICCRTS), Cambridge, United Kingdom, September 26-28, 2006. Paper Number: I-061. http://www.dodccrp.org/events/11th_ICCRTS/html/presentations/061.pdf

Congedo, L. (2018). Semi-Automatic Classification Plugin Documentation. Free Software Foundation. https://doi.org/10.13140/RG.2.2.29474.02242/1.

Cornell, P. (2020). Town and Fortification in the Early Modern. A complex relation-ship. FORTMED 2020. X, 585–92. Universitat Politàcnica de València. https://doi.org/10.4995/FORTMED2020.2020.11525.

Creosote Treated Timber, What you need to know, Wood Protection, West Yorkshire LONZA.

Davies, William J., Mags D. Adams, Neil S. Bruce, Rebecca Cain, Angus Carlyle, Peter Cusack, Deborah A. Hall, et al. (febbraio 2013) «Perception of Soundscapes: An Interdisciplinary Approach». Applied Acoustics 74, n. 2: 224–31. https://doi.org/10.1016/j.apacoust.2012.05.010.

Delvosalle, C., Fiévez, C., Pipart, A., Fabrega, J., Planas, E., Christou, M., & Mushtaq, F. (2005). Identification of reference accident scenarios in SEVESO establishments, Reliability Engineering & System Safety, Volume 90, Issues 2–3, Pages 238-246, https://doi.org/10.1016/j.ress.2004.11.003. https://www.sciencedirect.com/science/article/pii/S0951832004002625

Delvosalle, C., Fievez, C., Pipart, A., Casal Fabrega, J., Planas, E., Christou, M., et al. (2005). Identification of reference accident scenarios in SEVESO establishments. Reliability Engineering and System Safety, 90, 238e246.

Di Loreto, S., Serpilli, F., & Lori, V. (2022). Soundscape Approach in the Seaport of Ancona: A Case Study. Acoustics, 4(2), 492–516. https://doi.org/10.3390/acoustics4020031.

El Sayed, MD, MPH, FAAEM, FACEP, M., Zgheib, MD, H., Bachir, MPH, R., & Ghaddara, MD, H. (2015). Description of blast injuries and predictors of admission to hospital in blast victims in an urban civilian setting. American Journal of Disaster Medicine, 10(4), 309-315. doi: https://doi.org/10.5055/ajdm.2015.0213.

Ghasemi, & A., Nourai, F., (2017). A framework for minimizing domino effect through optimum spacing of storage tanks to serve in land use planning risk assessments,
Safety Science, Volume 97. https://doi.org/10.1016/j.ssci.2016.04.017.
Gilmore S., Saleem A., Dewan A., 2015. Effectiveness of DOS (Dark-Object Subtraction) method and water index techniques to map wetlands in a rapidly urbanising megacity with Landsat 8 data. Department of Spatial Sciences Curtin University, Perth, WA.
Herman S. Wolk. 1962 Deterrence Under Fire. Air Force. http://www.dec.ny.gov/regulations/regulations.html.
Chander, G., Markham, B., & Helder, D. (2009). Summary of current radiometric calibration coefficients for Landsat MSS, TM, ETM+, and EO-1 ALI sensors, Remote Sensing of Environment, Volume 113, Issue 5, Pages 893-903, https://doi.org/10.1016/j.rse.2009.01.007. https://www.sciencedirect.com/science/article/pii/S0034425709000169
Moretti, Beatrice. (2017). PORTUALITY XXI / research status WIP. https://doi.org/10.13140/RG.2.2.17143.21926.
NFPA 15 - Standard for Water Spray Fixed Systems for Fire Protection, (2007). National Fire Protection Association. https://www.nfpa.org/
NFPA 30 - Flammable and Combustible Liquids Code, (2012). National Fire Protection Association. https://www.nfpa.org/
UN-Habitat. (2020). Preserving historic Lebanese homes through heritage conservation and urban renewal.
Vermote, E., Justice, C., Claverie, M., Franch, B. (2016). Preliminary analysis of the performance of the Landsat 8/OLI land surface reflectance product, Remote Sensing of Environment, Volume 185, Pages 46-56, DOI: https://doi.org/10.1016/j.rse.2016.04.008. https://www.sciencedirect.com/science/article/pii/S0034425716301572
White, R., 2002. Analytical methods for determining fire resistance of timber members. Chapter 4 of Section 4, SFPE Handbook of Fire Protection Engineering, 3rd Edition. Quincy, MA: National Fire Protection Association. pp. 4-257 to 4-273.
Zhan, X.-K., You, Z.-H., Li, L.-P., Li, Y., Wang, Z., & Pan, J. (2020). Using Random Forest Model Combined With Gabor Feature to Predict Protein-Protein Interaction From Protein Sequence. Evolutionary Bioinformatics. DOI: https://doi.org/10.1177/1176934320934498.
Transportation Dept. (U.S.). Research and Special Programs Administration, (2000). Emergency Response Guidebook: A Guidebook for First Responders During the Initial Phase of a Dangerous Goods/Hazardous Materials Incident. Research and Special Programs Administra.